Int. J. Electrochem. Sci., 13 **(2018)** 9131 – 9144, doi: 10.20964/2018.09.62

International Journal of
ELECTROCHEMICAL
SCIENCE
www.electrochemsci.org

Investigation of Inhibition Effect of Ketoconazole on Mild Steel Corrosion in Hydrochloric Acid

Haolong Yang[1,*], *Ming Zhang* [2,3,*], *Ambrish Singh*[3,4]

[1]School of Petroleum and Natural Gas Engineering, Chongqing University of Science and Technology, Chongqing-401331, China.
[2]Sichuan Institute Research of Building Materials, Chengdu-610000, Sichuan, China.
[3]State Key Laboratory of Oil and Gas Reservoir Geology and Exploitation, Southwest Petroleum University, Chengdu-610500, China.
[4]School of Materials Science and Engineering, Southwest Petroleum University, Chengdu-610500, China.
[*]E-mail: haolongyang2000@sina.com

Received: 19 May 2018/ *Accepted:* 3 July 2018 / *Published:* 5 August 2018

Inhibition behavior of a common drug Ketoconazole with IUPAC name as **(**1-[4-(4-{[(2*R*,4*S*)-2-(2,4-Dichlorophenyl)-2-(1*H*-imidazol-1-ylmethyl)-1,3-dioxolan-4-yl]methoxy}phenyl)piperazin-1-yl]ethan-1-one) was investigated for mild steel corrosion using weight loss, electrochemical impedance spectroscopy (EIS), potentiodynamic polarization and theoretical methods. The surface was observed through scanning kelvin probe (SKP), atomic force microscopy (AFM), and scanning electron microscopy (SEM). The drug showed the maximum efficiency of 97% at 100 ppm through weight loss method, 93% through polarization method and 94% through EIS method. The equal relocation of the anodic and cathodic regions indicated that the drug belong to mixed type inhibitor category. Theoretical computations in addition to the experimental results supported the protective action of inhibitor on the mild steel surface due to adsorption.

Keywords: Ketoconazole, SKP, DFT, EIS, Polarization, AFM, Inhibitor

1. INTRODUCTION

Mild steel is utilized in pickling, acidization and various other manufacturing units due to its low cost and ease of availability. The mechanical properties of mild steel are superior and add extra advantage for it worldwide applications. Mild steel can easily give rise to rust after oxidation due to humid and corrosive environment. The reactivity of the mild steel with environment makes it very

vulnerable to threats. The steel can get deteriorated after reacting with its surrounding environment and can develop several pits, cracks and rough patches on the surface [1]. Oil and petroleum industries regularly use hydrochloric and sulphuric acids to eliminate scale and rust present on the surface of the steel. This process removes rusts and scale from the steel surface but due to chemical reaction pits and cracks are developed leading to big failures.

There are several methods to mitigate corrosion of the mild steel. Implementation of inhibitors is one of them as this is very easy to handle, and the subsequent cost is very low [2-4]. Chemical substances are used as inhibitors in optimum concentration to mitigate the corrosion reaction. These chemical compounds are affluent in heteroatom containing groups (N, O, and S), multiple bonds, and aromatic rings [5]. These groups donate their extra pair of electrons to the available d-orbital of Fe (iron) in the steel and form a complex on the surface. This complex serves as a protective layer and keeps the corrosive media away from the metal surface [6, 7]. The environmental regulatory bodies have strict regulations regarding the use of toxic chemical compounds. So, use of drugs is an effective solution as they are non-toxic and emphasis on several drugs as corrosion inhibitor is given in recent times [8-15].

Ketoconazole is a less toxic and effective drug synthesized from Imidazole. Its antifungal tablets are used basically to treat infections due to fungi. Ketoconazole is a commercial medicine which is also used to treat dandruff and is included in shampoos. The wide applications of Ketoconazole include creams, soaps and conditioners which are used almost in day to day life by everyone. After recommendation a ban was imposed on oral tablets are and now it is banned in some countries (Europe, Australia, China) due to liver problems detected in people. The current research work aims at the study of Ketoconazole as corrosion inhibitor of mild steel in 1M HCl using weight loss, electrochemical and theoretical methods.

2. EXPERIMENTAL

2.1. Method and Materials

The mild steel samples were used with composition (wt. %): 0 .076% C, 0.192% Mn, 0.012% P, 0.026% Si, 0.050% Cr, 0.023% Al, 0.123% Cu and balance Fe [16]. The dimension of the mild steel coupons used for weight loss studies were 2.5 cm × 2 cm × 0.025 cm and for electrochemical studies 8 cm × 1 cm × 0.025 cm dimensions were used. The samples were carefully covered with epoxy resin exposing 1 $cm^2$for the experiments. The 1M HCl solution was prepared from chemical grade hydrochloric acid by adulterating it with distilled water. All the tests were executed in static environment and in unstirred solutions.

Ketoconazole were commercially obtained as generic tablets manufactured by the Cipla Ltd., Anantpur, Haridwar. The compound is in its pure condition, with molecular formula ($C_{26}H_{28}Cl_2N_4O_4$) and molecular mass (531.43). Its elemental configuration is shown in Figure1.

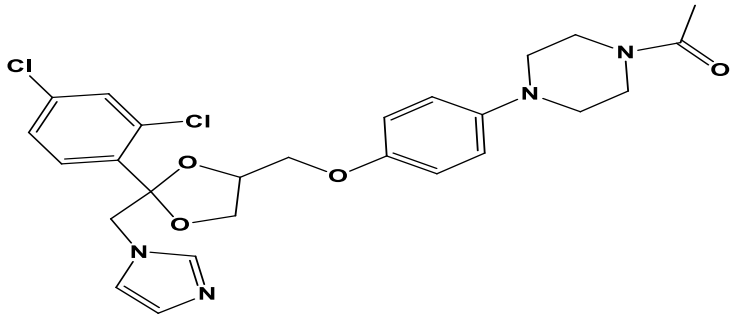

Figure 1. Molecular structure of Ketoconazole **(**1-[4-(4-{[(2*R*,4*S*)-2-(2,4-Dichlorophenyl)-2-(1*H*-imidazol-1-ylmethyl)-1,3-dioxolan-4-yl]methoxy}phenyl)piperazin-1-yl]ethan-1-one).

2.2. Weight Loss measurement

The weight loss tests were executed in conical flasks which were kept in an oven at a room temperature for 3 hours. The polished mild steel samples were engrossed in 1M HCl with and without Ketoconazole inhibitor. The samples were weighed before and after immersion in the solution to get the difference in the weight of the metal samples. The corrosion tests were performed on triplicate samples and their mean corrosion rate was calculated. The following equation was used to calculate the corrosion rate (C_R) [17]:

$$C_R\,(\mathrm{mm/y}) = \frac{8.76W}{atD} \qquad (1)$$

where W is the weight loss of mild steel specimens, a total area of mild steel specimen, t is the immersion time (3 hours) and D is density of mild steel in (gcm^{-3}). The inhibition efficiency (η%) of the inhibitor was calculated as follows [18]:

$$\eta\% = \frac{C_R - {}^{inh}C_R}{C_R}\ \mathrm{X}\ 100 \qquad (2)$$

where C_R and ${}^{inh}C_R$ are the corrosion rates of mild steel with and without Ketoconazole inhibitor, respectively [18].

2.3. Electrochemical Tests

Electrochemical tests were done to study the corrosion behavior of mild steel in the existence and deficit of Ketoconazole. The traditional assembly of three electrode cell was used and connected to Gamry workstation equipped with Echem analyst software to fit the results. Potentiodynamic curves were acquired by transforming the potential from −250 V to +250 mV at a scan rate of 1 mV s^{-1}. EIS measurements were executed under potentiostatic conditions in a frequency range from 100 kHz to 0.01 Hz, with amplitude of 10mV AC signal. An immersion period of 30 minutes was employed before the test to attain a stable potential [19].

2.4. Scanning Kelvin Probe

Bard and co-workers developed SKP to detect the micro electrochemical changes at the metal surface [20]. This technique can detect the uniform corrosion as well as can give influential results about the localized corrosion. The technique is very versatile and comes with varied options of research modes to be selected depending on the metal-solution metal-probe behavior[21].The assembly of electrochemical cell was similar as used in the traditional electrochemical tests having working, auxiliary and reference electrode. SKP experiments were executed using Princeton workstation equipped with Versa scan software (USA). The microelectrode had a silver Pt/Ir tip with a width of around 10 µm and vibrated with 30µm of amplitude, at an average distance of 100µm over the surface [22].

2.5. Scanning Electron Microscopy

The changes on the metal surface in deficient and in presence of Ketoconazole were explored through SEM. Before the test the metal samples were engrossed in the corrosive solution with and without inhibitor. The samples were washed with alcohol to remove any salt or by-products on the surface. The samples were then dehydrated at room temperature and kept in desiccator. TESCAN VEGA and Zeiss were used to record the surface changes on the metal surface after being exposed to the corrosive media [23].

2.6 Atomic Force Microscopy

The N80 metal samples were immersed in the corrosive solution before being exposed to the AFM test. The metal sample was then sanitized with water, washed with alcohol and dried out carefully. AFM tests were performed using a NT-MDT multimode AFM workstation [24].

2.7. Theoretical calculations

Quantum chemical parameters were evaluated using density function theory (DFT) method. The essential condition chosen for all the tests was B3LYP with electron source set 6-31G* (d, p) for every atoms. Theoretical computations were carried out using Gaussian 9.0 and Gauss view software. Different parameters were obtained and analyzed including highest occupied molecular orbital (E_{HOMO}), lowest unoccupied molecular orbital ($E_{LUMO)}$, total energy ($\Delta E_{LUMO\text{-}HOMO)}$) [25]. All the parameters were calculated for neutral Ketoconazole inhibitor and protonated inhibitor to distinguish between the results obtained.

3. RESULTS AND DISCUSSION

3.1. Weight loss measurements

The weight loss tests were conducted in 1M HCl with and without Ketoconazole inhibitor for 3 hours. The inhibition effectiveness was found to amplify when the absorption of the inhibitor was

increased at higher concentration. At 100 ppm concentration of the inhibitor maximum efficiency of 97% was obtained and no further significant changes were noticed after increasing the concentration [26]. So, we considered 100 ppm as the optimum concentration for all the tests. Table 1 shows the results for mild steel in presence and lack of inhibitor.

Table 1. Weight loss results for mild steel in 1M HCl with and without inhibitor.

Inhibitor concentration(ppm)	Weight loss (mg cm^{-2})	η%	C_R (mm/y)	θ
Blank	20.0	-	74.2	-
25	1.5	57.5	5.6	0.92
50	1.1	70.5	4.0	0.94
100	0.6	86.0	2.2	0.97

3.2. Electrochemical measurements

3.2.1. Electrochemical impedance spectroscopy (EIS)

The Nyquist plots and equivalent circuit are shown in Figure 2 for mild steel in 1M HCl solution. The consequent Bode and phase angle graphs are depicted in Figure 3 [27].

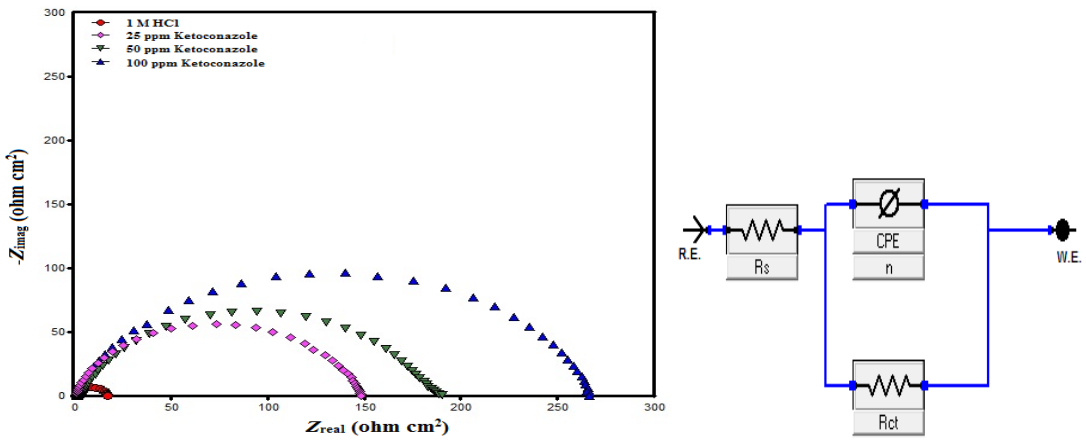

Figure 2. Nyquist plot and Equivalent circuit for mild steel in 1M HCl with and without Ketoconazole.

The impedance spectra for corrosive solution were computed by using the corresponding circuit to fit the tests outcome (Figure 2) that was used before to elucidate the corrosion process at interface [28, 29]. The circuit contains R_s as the solution resistance, R_{ct} as the charge transfer resistance, and CPE as a constant phase elementand double layer capacitance (C_{dl}) in series with solution resistance (R_s) [30].

$$C_{dl} = Y_0(\omega_{max})^{n-1} \quad (3)$$

Where Y_0 is CPE coefficient, n represents the phase shift, ω be the frequency. The results obtained are tabulated in (Table 2).

For electrochemical impedance the effectiveness of Ketoconazole was evaluated using the equation below:

$$\eta\% = \frac{R_{ct(inh)} - R_{ct}}{R_{ct(inh)}} \times 100 \quad (4)$$

where $R_{ct(inh)}$ and R_{ct} represent the values of charge transfer resistance with and without Ketoconazole in 1M HCl correspondingly [31].

Table 2. Electrochemical impedance parameters and inhibition efficiency of Ketoconazole in 1M HCl.

Inhibitor concentration(ppm)	R_{ct} (Ω cm^2)	n	Yo ($10^{-6}\Omega^{-1}$ cm^{-2})	C_{dl} (μF cm^{-2})	η%
Blank	16.3	0.845	197.6	100.6	-
25	150.8	0.867	58.9	72.1	89
50	198.9	0.871	96.4	42.5	92
100	267.3	0.872	67.7	12.6	94

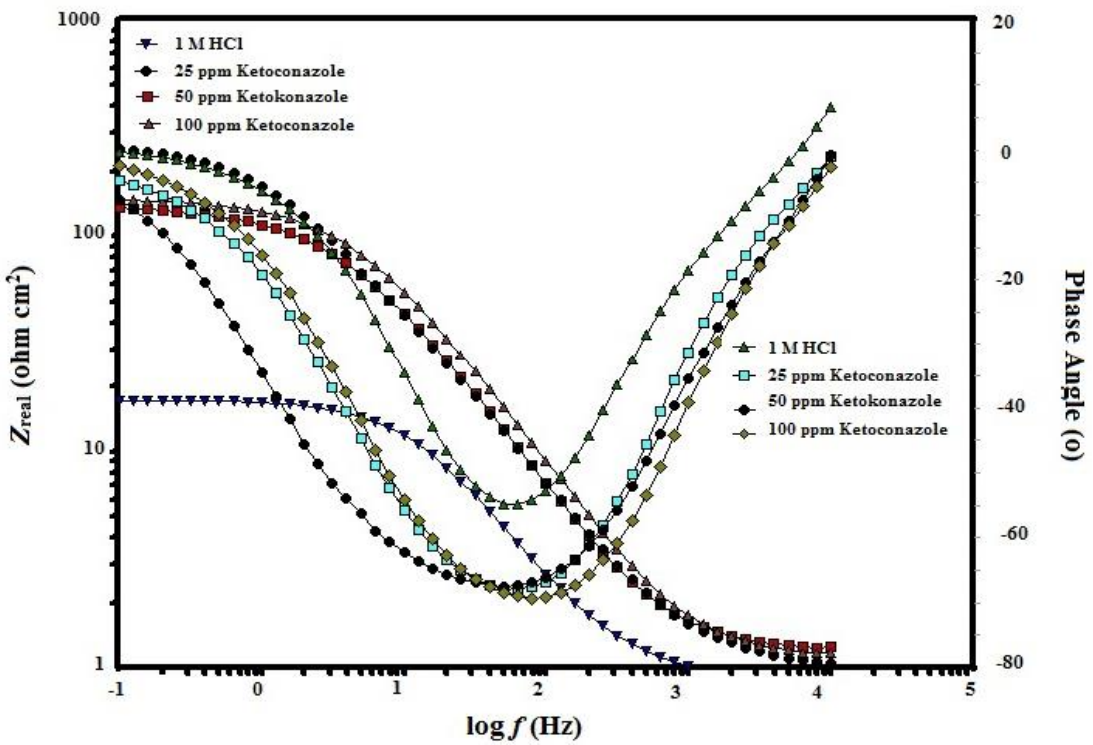

Figure 3. Bode-impedance and Phase angle plots for mild steel in 1M HCL and different concentration of Ketoconazole

The charge transfer resistance values enlarge as the absorption of Ketoconazole was increased. This may be due to the increased number of inhibitor molecules covering the mild steel surface and resisting the corrosive solution. Although, the overall shape of the Nyquist curves did not change they showed a wider diameter for higher concentration of inhibitor [32]. The inhibitor molecules cover the reactive locations on the metal surface and do not allow the 1M HCl solution to penetrate to the surface. This results in a wider diameter and higher values of charge transfer resistance. The values of capacitance showed a lesser value at higher concentration due to the inversely proportional nature of local dielectric and electrical double layer [33].

$$C_{dl} = \frac{\varepsilon \varepsilon_{\circ} A}{d} \tag{5}$$

where ε_0 be the constant, ε represents the local dielectric constant, d be the thickness of the double layer, and A is the surface area of the mild steel. Reduction in capacitance is due to adsorption of Ketoconazole on mild steel surface as it is inversely proportional to the width of the double layer [34].

3.2.2. Potentiodynamic polarization measurements

The polarization plots of metal samples in 1M HCl are exposed in Figure 4 [35]. Corrosion potential (E_{corr}), corrosion current density (I_{corr}), anodic and cathodic slopes (β_a and β_c) acquired from the graphs are tabulated in Table 3. The efficiency of Ketoconazole was evaluated with the help of the equation given below:

$$\eta\% = \frac{I_{corr} - I_{corr(inh)}}{I_{corr}} \times 100 \tag{6}$$

where I_{corr} and $I_{corr(inh)}$represent the corrosion current density of mild steel [36].

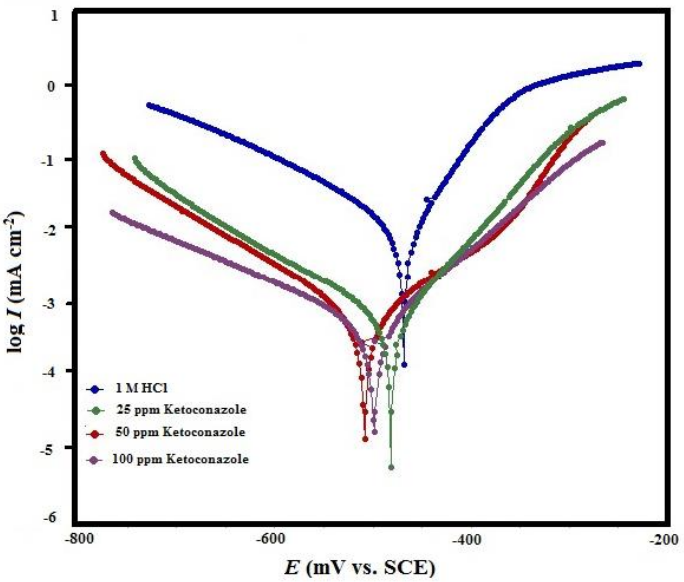

Figure 4. Polarization graph of mild steel in 1M HCl with and without Ketoconazole.

With increase in the concentration of Ketoconazole there is decline in I_{corr} values. This decline is

due to the reduction in the rate of corrosion. The anodic and cathodic (β_a and β_c) values obtained from the potentiodynamic plots show a shift in both directions and indicate that the addition of Ketoconazole does not alter the means of oxidization [37]. If the value of $-E_{corr}$ is more than 85 mV then the inhibitor can be categorized into anodic or cathodic type [38]. The data acquired for Ketoconazole illustrate values between 35-40 mV of corrosion potential (E_{corr}) that suggests that it belongs to the mixed type category [39]. The efficiency of Ketoconazole was 93% at 100 ppm concentration contrast to the 1M HCl solution which suggest the formation of metal-TF complex at the interface due to adsorption [40].The Ketoconazole gets adsorbed on the mild steel surface and guards it from 1M HCl solution thereby mitigating corrosion reaction [41].

Table 3. Polarization data for mild steel in 1M HCl in absence and presence of different concentration of Ketoconazole

	Potentiodynamic Polarization				
Inhibitor concentration(ppm)	E_{corr} (mVvs SCE)	β_a (mV/dec)	$-\beta_c$ (mV/dec)	I_{corr} ($\mu A\ cm^2$)	η%
Blank	-469	47	83	603	-
25	-509	137	41	84	86
50	-482	73	128	59	89
100	-480	87	132	42	93

3.3. Scanning Kelvin Probe (SKP) method

The SKP method furnishes helpful data about the localized and nano-corrosion development on the metal surface with the help of a vibrating probe [22, 42]. Figure 5 reveal that at the period of contact the potential of the mild steel tends to be irregular without Ketoconazole due to the commencement of deterioration causing fractures and fissures on the surface (Figure 5a).

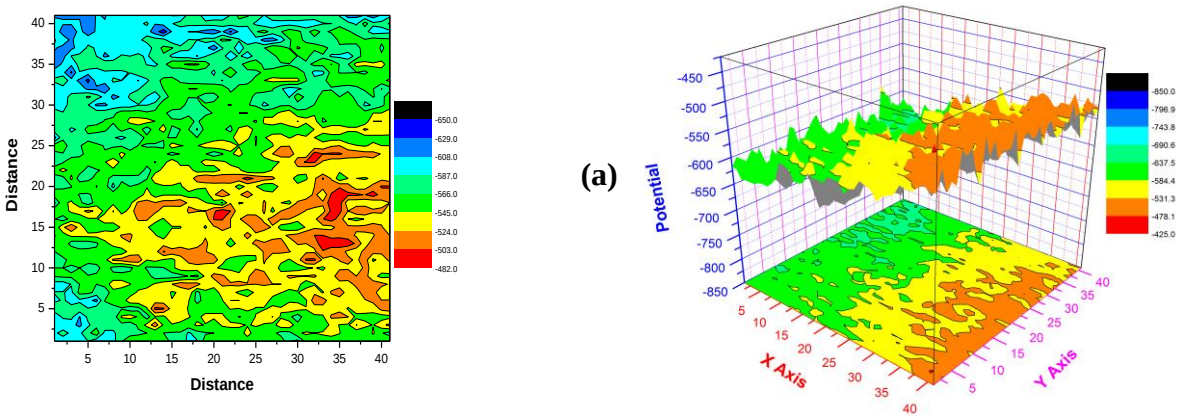

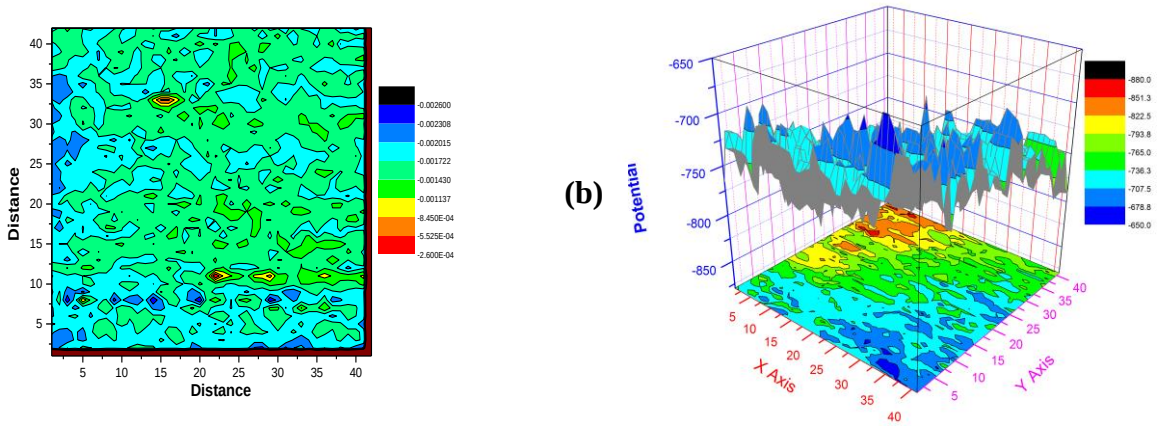

Figure 5. SKPgraph of mild steel in 1M HCl with and without Ketoconazole.

The progress of the cathodic motion on the surface having Ketoconazole inhibitor is probably due to the time utilized by the 1M HCl solution to enter through the inhibitor complex at the metal surface as shown in Figure 5b [43]. The surface was more anodic without inhibitor and more cathodic in presence of inhibitor film which defends our previous results of weight loss, EIS and potentiodynamic studies.

3.4. Scanning Electron Microscopy

SEM photographs with and without Ketoconazole are shown in Figure 6a, 6b. A damaged and rough mild steel surface can be seen in Figure 6a in absence of inhibitor. The corrosion of the metal surface led to cracks, pits and dents which are visible in the figure [44]. Nonetheless, a smooth and less corroded surface was observed in Figure 6b for mils steel surface in presence of Ketoconazole inhibitor. The surface was less damaged without pits and cracks. This can be accredited to the superior action by Ketoconazole inhibitor on mild steel surface that obstructed the corrosive media by forming a film/complex on the metal surface [45].

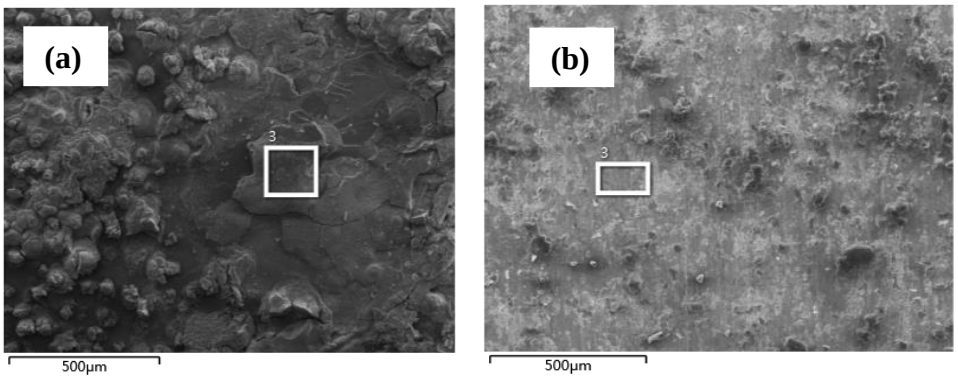

Figure 6. SEMgraph of mild steel in 1M HCl with and without Ketoconazole.

3.5. Atomic Force Microscopy

The 3-D pictures of AFM with and without Ketoconazole inhibitor is shown in Figure 7a, 7b. As can be seen from Figure 7a the metal surface is strongly damaged without inhibitor and the roughness level is very high. On the other hand, in presence of Ketoconazole inhibitor the roughness level is reduced and the surface appears to be smooth as shown in Figure 7b [46].

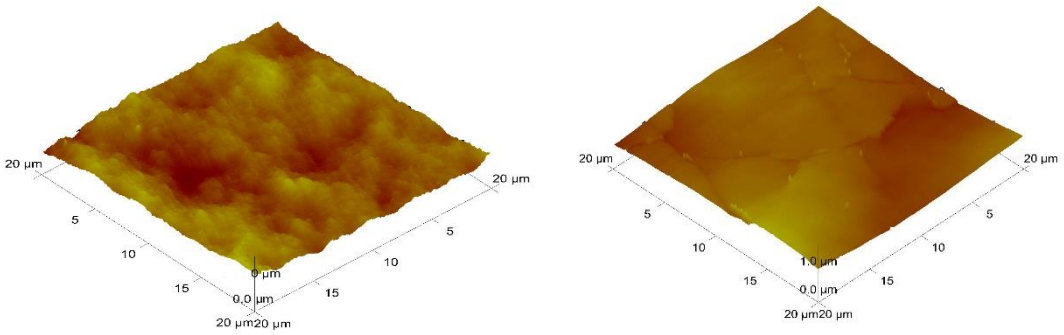

Figure 7.AFMgraph of mild steel in 1M HCl with and without Ketoconazole.

3.6 Adsorption Isotherm

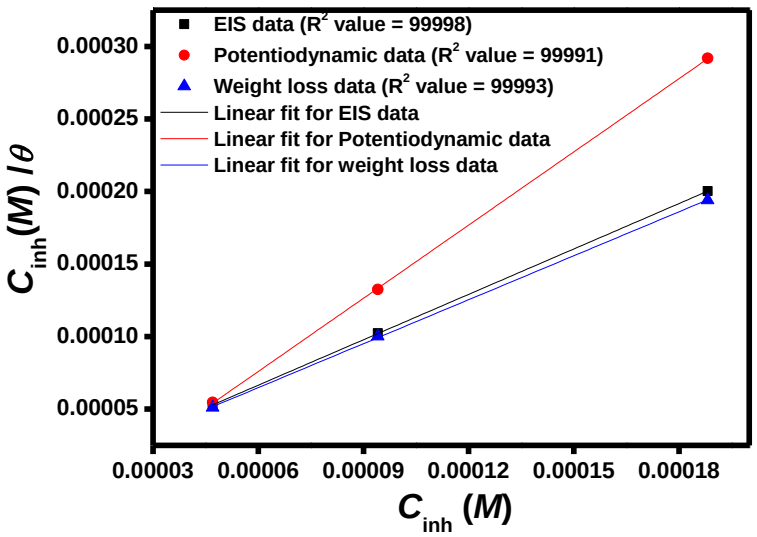

Figure 8. Langmuir adsorption isotherm graph of mild steel in 1M HCl with Ketoconazole.

To study the adsorption behavior of the Ketoconazole molecule on the mild steel surface in 1M HCl solution different adsorption isotherms were tried to fit the data. Among all of them Langmuir adsorption isotherm gave the best fit with a straight line for weight loss, EIS and potentiodynamic polarization data. The equation used to establish the Langmuir isotherm is as under:

$$\frac{C_{inh}}{\theta} = \frac{1}{K_{ads}} + C_{inh} \qquad (8)$$

where C_{inh} is the inhibitor concentration, K_{ads} is the adsorptive equilibrium constant and θ is the surface coverage. Concentration of the molecule (C_{inh} (M)) can be plotted against the concentration by surface coverage (C_{inh} (M)) /θ) to get the graph for the Langmuir adsorption as shown in Figure 8. The regression coefficient value for weight loss (0.99993), Potentiodynamic polarization (0.99991) and EIS (0.99998)were almost close to unity suggesting the good fit of the isotherm.

3.7. Quantum Chemical Computations

Theoretical data for Ketoconazole such as E_{HOMO} (high occupied molecular orbital energy), and E_{LUMO} (lowest unoccupied molecular orbital energy) were computed and the results obtained are provided in Table 4 [47]. The structure of Ketoconazole after optimization and frontier molecular orbital of neutral and protonated Ketoconazole molecule are exposed in Figure 9.

Table 4. Calculated quantum chemical parameters of studied Ketoconazole drug

TE	E_{HOMO}	E_{LUMO}	ΔE	IE	χ	ΔN
K-neutral	-1.387744	-1.053184	0.33456	1.387744	1.220464	10.7590148
K-protonated	-4.833984	-1.030608	3.803376	4.833984	2.932296	0.49632327

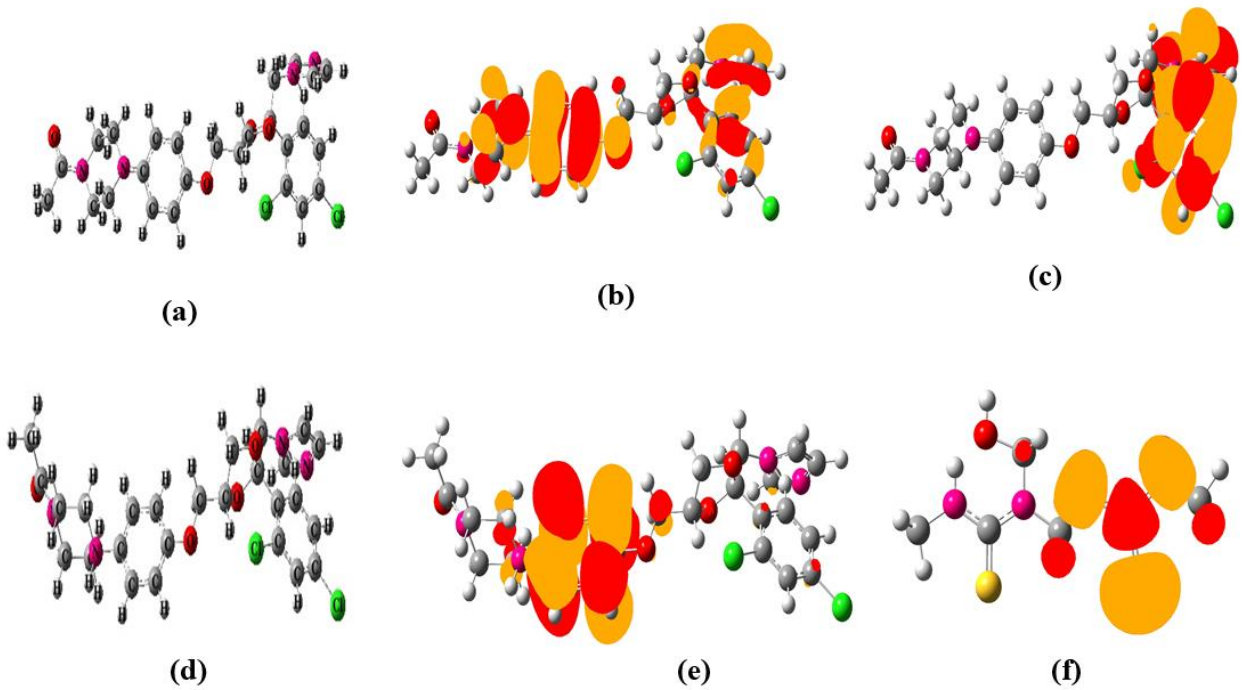

Figure 9.(a)Optimized molecular structure (b) HOMO (c) LUMO for neutral Ketoconazole and (d)Optimized molecular structure (e) HOMO (f) LUMO for protonated Ketoconazole.

The efficiency of Ketoconazole is directly proportional to the energy gap (ΔE), lower the energy gap higher the efficiency [48]. E_{HOMO} represents the electron donating ability of the Ketoconazole molecules; therefore molecules with higher E_{HOMO} values prove to be better electron donors. E_{LUMO}

represents the propensity of the Ketoconazole molecules to accept electrons so; the lesser value of E_{LUMO} represents the likelihood to accept electrons [49].

Additionally, it could be scrutinized from table 4 that the E_{HOMO} data of protonated Ketoconazole is contrast to the neutral one. Consequently, protonated Ketoconazole has smaller electron donating capacity than neutral. On the other hand, the E_{LUMO} values for Ketoconazole inhibitor showed additional negative values than neutral, signifying that protonated Ketoconazole has superior capability to accept electron as compared to neutral one [50]. The calculated values of ΔN expose that each and every ΔN values in neutral Ketoconazole is positive and so electron shift occurs from Ketoconazole to mild steel. As a result, overall after protonation the theoretical data have been varied which consequences the HOMO and LUMO values contrast to the neutral Ketoconazole values [51].

3.8. Mechanism of adsorption and inhibition

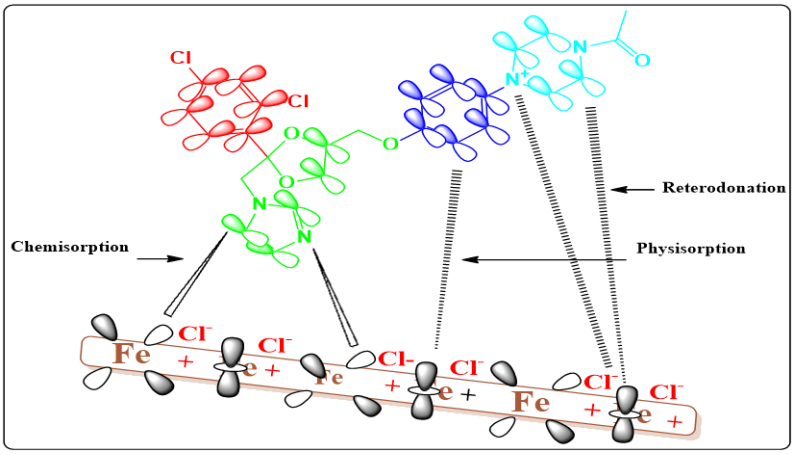

Figure 10. Mechanism of corrosion mitigation by Ketoconazole drug.

Ketoconazole mitigates corrosion by dominating both the anodic and cathodic reactions. In solutions containing acids, Ketoconazole subsists as protonated species [52]:

$$\left[C_{26}H_{28}Cl_2N_4O_4\right]+xH^+ \rightarrow \left[C_{26}H_{28+x}Cl_2N_4O_4\right]^{x+}$$

The mechanism of adsorption (chemical and physical) of Ketoconazole on mild steel surface can be explained by the subsequent ways:(i) the protonated molecule subsides the hydrogen evolution by adsorbing on the cathodic regions, (ii) the heteroatoms in the Ketoconazole molecule donate their extra lone pair of electron, and (iii) the π-electron of aromatic rings form bonds with the steel surface decreasing the anodic dissolution [53] as shown in Figure 10. Therefore, the metal-inhibitor complex formed by Ketoconazole at the interface helps in mitigating corrosion of the mild steel in hydrochloric acid solution [54].

4. CONCLUSIONS

(a) Ketoconazole is an excellent inhibitor for mild steel in 1M HCl.

(b) Polarization figure specified that Ketoconazole belong to mixed-type category. The

-E_{corr} values obtained were less than 85 mV.

(c) SKP, SEM and AFM depicted that Ketoconazole mitigated corrosion by adsorbing on the mild steel surface.

(d) Theoretical computation well supported the data obtained by weight loss, EIS and potentiodynamic studies.

ACKNOWLEDGEMENT
Authors are thankful to the Sichuan 1000 talent fund, Chongqing University and Southwest Petroleum University for financial assistance.

References

1. M. A. Quraishi, D.Jamal, *Mater. Chem. Phys*., 68 (2001) 283.
2. Z. Tao, S. Zhang, W. Li, B. Hou, *Corros. Sci.*, 51 (2009) 2588.
3. M.M. Solomon, S.A. Umoren, I.I. Udosoro, A.P. Udoh, *Corros. Sci.*, 52 (2010) 1317.
4. H. Ashassi-Sorkhabi, S.A. Nabavi-Amri, *Electrochim. Acta*, 47 (2002) 2239.
5. H. Ashassi-Sorkhabi, B. Shaabani, D. Seifzadeh, *Electrochim. Acta*, 50 (2005) 3446.
6. Ambrish Singh, K.R. Ansari, Jiyaul Haque, Parul Dohare, Hassane Lgaz, Rachid Salghi, M.A. Quraishi, *J. Taiwan Inst. Chem. E*., 82 (2018) 233.
7. A. Singh, K. R. Ansari, X. Xu, Z. Sun, A. Kumar, Y.Lin, (2017) *Sci. Report*., 7 (2017) DOI:10.1038/s41598-017-13877-0.
8. I. Ahamad, M.A. Quraishi, *Corros. Sci.*, 52 (2010) 651.
9. G. Gece, *Corros. Sci*., 53 (2011) 3873.
10. S.E. Nataraja, T.V. Venkatesha, H.C. Tandon, B.S. Shylesha, *Corros. Sci*., 53 (2011) 4109.
11. I. Ahamad, R. Prasad, M.A. Quraishi, *Corros. Sci*., 52 (2010) 3041.
12. I.B. Obot, N.O. Obi-Egbedi, *Corros. Sci.*, 52 (2010) 198.
13. P. Xuehui, R. Xiangbin, K. Fei, X. Jiandong, H. Baorong, *Chinese J. Chem. Eng.*,18 (2010) 337.
14. M.M. El-Naggar, *Corros. Sci*., 49 (2007) 2226.
15. I. Ahamad, M.A. Quraishi *Corros. Sci*., 52 (2010) 656.
16. A. Singh, K.R. Ansari, A. Kumar, W. Liu, C. Songsong, Y. Lin, *J. Alloys Comp.*,712 (2017)121.
17. A. Singh, K.R. Ansari, J. Haque, P. Dohare, H. Lgaz, R. Salghi, M.A.Quraishi, *J. Taiwan Inst. Chem. E.*, 82 (2018) 233.
18. A. Singh, Y. Lin, E. E. Ebenso, W. Liu, B. Huang, *Int. J. Electrochem. Sci*., 9 (2014) 5993.
19. A. Singh, E. E. Ebenso, M. A. Quraishi, Y. Lin, *Int. J. Electrochem. Sci*., 9 (2014) 7495.
20. B. M. Quinn, I. Prieto, S. K. Haram, A. J. Bard, *J. Phys. Chem. B.*, 105 (2001) 7474.
21. A. J. Bard, G. Denuault, C. Lee, D. Mandler, D. O. Wipf, *Acc. Chem. Res*., 23 (1990) 357-363.
22. Hongwei Feng, Ambrish Singh, Yuanpeng Wu, Yuanhua Lin, (2018) DOI: 10.1039/c8nj01676c.
23. A. Singh, Y. Lin, W.Liu, S. Yu, J.Pan, C. Ren, D. Kuanhai, *J. Ind. Eng. Chem*., 20 (2014) 4276.
24. Ambrish Singh,Mohd Talha, Xihua Xu, Zhipeng Sun, Yuanhua Lin, *ACS Omega*, 2 (2017) 8177.
25. Gaussian 09, Revision E.01, M.J. Frisch, G.W. Trucks, H.B. Schlegel, G.E. Scuseria, M.A. Robb, J.R. Cheeseman, Jr. J.A. Montgomery, T. Vreven, K.N. Kudin, J.C. Burant, J.M. Millam, S.S. Iyengar, J. Tomasi, V. Barone, B. Mennucci, M. Cossi, G. Scalmani, N. Rega, G.A. Petersson, H. Nakatsuji, M. Hada, M. Ehara, K. Toyota, R. Fukuda, J. Hasegawa, M. Ishida, T. Nakajima, Y. Honda, O. Kitao, H. Nakai, M. Klene, X. Li, J.E. Knox, H.P. Hratchian, J.B. Cross, V. Bakken, C. Adamo, J. Jaramillo, R. Gomperts, R.E. Stratman, O. Yazyev, A.J. Austin, R. Cammi, C. Pomelli, J.W. Ochterski, P.Y. Ayala, K. Morokuma, G.A. Voth, P. Salvador, J.J. Dannenberg, V.G. Zakrzewski, S. Dapprich, A.D. Daniels, M.C. Strain, O. Farkas, D.K. Malick, A.D. Rabuck, K. Raghavachari, J.B. Foresman, J.V. Ortiz,Q. Cui, A.G. Baboul, S. Clifford, J. Cioslowski, B.B.

Stefanov, G. Liu, Liashenko, A .P. Piskorz, I.Komaromi, R.L. Martin, D.J. Fox, T. Keith, M.A. Al-Laham, C.Y. Peng, A. Nanayakkara, M. Challacombe, P.M.W. Gill, B. Johnson, W. Chen, M.W. Wong, C. Gonzalez, J.A. Pople, Gaussian, Inc., Wallingford CT, (2009)
26. A. Singh, A.K. Singh, M. A. Quraishi, *Open Electrochemi. J.*, 2 (2010) 51.
27. M. A. Quraishi, A. Singh, V. K. Singh, D. K. Yadav, A. K. Singh, *Mater. Chem. Phys.*, 122 (2010) 114.
28. I.B. Obot, N.O. Obi-Egbedi, *Corros. Sci*., 52 (2010) 198.
29. Ambrish Singh, K. R. Ansari, M. A. Quraishi, Hassane Lgaz and Yuanhua Lin, *J. Alloys Comp*., 762 (2018) 347.
30. X. Li, S. Deng, H. Fu, *Corros. Sci*., 53 (2011) 3241.
31. I. Ahamad, R. Prasad, M.A. Quraishi, *Corros. Sci.*, 52 (2010) 3033.
32. A. Singh, I. Ahamad, M. A. Quraishi, *Arab. J. Chem.*, 9 (2016) S1584.
33. A. Singh, Y. Lin, W. Liu, D. Kuanhai, J. Pan, B. Huang,C. Ren, D. Zeng, *J. Tai. Inst. Chem. E.*, 45 (2014) 1918.
34. A. Singh, I. Ahamad, V. K. Singh, M. A. Quraishi, J. Solid State Electrochem., 15 (2011) 1087.
35. P. Lowmunkhong, D. Ungtharatak, P. Sutthivaiyakit, *Corros. Sci*., 52 (2010) 30.
36. A. Singh, M. A. Quraishi, Res. Chem. Intermed. (2013) http://dx.doi: 10.1007/s11164-013-1398-3.
37. Xihua Xu, A. Singh, Z. Sun, K. R. Ansari, Y. Lin, *R. Soc. Open Sci*., 4 (2017) http://dx.doi.org/10.1098/rsos.170933.
38. Priyanka Singh, Ambrish Singh, M.A. Quraishi, *J. Taiwan Inst. Chem. E*., 60 (2016) 588.
39. A. Singh, Y. Lin, Chunyang Zhu, Y. Wu, E. E. Ebenso, *Chin. J. Pol. Sci.*, 33 (2015) 339.
40. A. Singh, Y. Lin, M. A. Quraishi, O. L. Olasunkanmi, O. E. Fayemi, Y. Sasikumar, B. Ramaganthan, I. Bahadur, I. B. Obot, A. S. Adekunle, M. M. Kabanda, E. E. Ebenso, Molecules, (2015) 2015122.
41. Ambrish Singh, Y. Lin, W. Liu, S. Yu, J. Pan, C. Ren, D. Kuanhai,*J. Ind. Eng. Chem.*, 20 (2014) 4276.
42. A. Singh, Yuanhua Lin, K. R. Ansari, M. A. Quraishi, E. E. Ebenso, Songsong Chen, W. Liu,*Appl. Surf. Sci.*, 359 (2015) 331.
43. W. Liu, A. Singh, Y. Lin, E. E. Ebenso, G. Tianhan, C. Ren, *Int. J. Electrochem. Sci*., 9 (2014) 5560.
44. A. Singh, Y. Lin, W. Liu, E. E. Ebenso, J. Pan, *Int. J. Electrochem. Sci.*, 8 (2013) 12884.
45. Ambrish Singh, Y. Lin, I. B. Obot, E. E. Ebenso, K. R. Ansari, M. A. Quraishi, *Appl. Surf. Sci*., 356 (2015) 341.
46. K.R. Ansari, M.A. Quraishi, Ambrish Singh, *J. Ind. Eng. Chem*., 25 (2015) 89.
47. A. Singh, Y. Lin, I. B. Obot. E. E. Ebenso, *J. Mol. Liq*., 219 (2016) 865.
48. K.R. Ansari, M.A. Quraishi, A. Singh, *Corros. Sci*., 79 (2014) 5.
49. I.B. Obot, S. Kaya, C. Kaya, B. Tüzün, *Physica E*., 80 (2016) 82.
50. E.E. Ebenso, T. Arslan, F. Kandemirli, N. Caner, I. Love, *Int. J. Quant. Chem.*, 110 (2010) 1003.
51. Ambrish Singh, K. R. Ansari, M. A. Quraishi, Hassane Lgaz, Yuanhua Lin, *J. Alloys Comp*., 762 (2018) 347.
52. A. Singh, Y. Lin, E. E. Ebenso, W. Liu, J. Pan, B. Huang, *J. Ind. Eng. Chem*., 24 (2015) 219.
53. Yuanhua Lin, Ambrish Singh, E. E. Ebenso, Yuanpeng Wu, Chunyang Zhu,H. Zhu,*J. Tai. Inst. Chem. Eng*., 46 (2015) 214.
54. K.R. Ansari, M.A. Quraishi, A. Singh, *Corros. Sci.*, 95 (2015) 62.